Journal of Oil, Gas and Petrochemical Technology 10(2): 125-137, Winter and Spring 2023

RESEARCH PAPER

Microscopic Modeling of Mass Transfer in LLE Systems Using VOF Approach: The Surface Tension Effects on Mass Transfer and Hydrodynamics

***Sepideh Roshdi*[1,*], *Norollah Kasiri*[2]**

[1]*Chemical Engineering Department, Faculty of Engineering, Urmia University, Urmia, Iran*

[2]*Computer Aided Process Engineering Center, School of Chemical Oil, and Gas Engineering, Iran University of Science & Technology, Narmak, Tehran, Iran*

ARTICLE INFO

Article History:
Received 22 February 2023
Revised 28 July 2023
Accepted 22 August 2023

Keywords:
Volume of fluid
mass transfer
Liquid-Liquid extraction
moving reference frame
surface tension
hydrodynamics

ABSTRACT

Liquid-liquid extraction is one of the main separation processes which has many applications in different industries. Among different influencing parameters on Liquid-liquid performance, the surface tension effect was investigated in the present study. The mass transfer of a single droplet was simulated using the volume of fluid approach coupled with a single-field mass transfer approach. Due to the high computational time, the moving reference frame approach was supplemented to computational codes in parallel processing mode assuming static droplet and moving zone. The results showed that with the reduction of surface tension coefficient, while the other parameters were kept constant, the regime change from spherical to oscillating occurred, the velocity decreased. In addition, along with an additional reduction in the surface tension coefficient, the droplet breakage happened. Despite a considerable reduction in terminal velocity, the reduction in mass transfer was not observed due to the interfacial area increase which enhanced mass transfer while velocity reduction negatively disturbed it. The concentration contour plots of droplets in various surface tension coefficients were reported in different droplet regimes starting from circulating to breakup.

How to cite this article
Roshdi S, Kasiri N., Microscopic Modeling of Mass Transfer in LLE Systems Using VOF Approach: The Surface Tension Effects on Mass Transfer and Hydrodynamics, Journal of Oil, Gas and Petrochemical Technology, 2023; 10(2): 125-137. DOI:10.22034/JOGPT.2023.386913.1112.

1. INTRODUCTION

The liquid-liquid extraction (LLE) process is applied in different industries such as refinery, petrochemical, pharmacy, food, nuclear, and biochemistry industry. The LLE performance in the industries is determined by the hydrodynamics and mass transfer of the million droplets. The extraction fraction, droplet shapes, and velocities are three factors to show the performance of the process. Any favorable/unfavorable variation in single droplet behavior affects the behavior of all droplets, consequently in process performance.

* *Corresponding Author Email: s.roshdi@urmia.ac.ir*

In the numerical approach, few studies have investigated influencing factors on LLE performance. When the surface tension coefficient (STC) of LLE systems depends on the solute concentration, the Marangoni convection effects appeared and caused enhanced mixing inside the droplets and enhanced mass transfer. The effect of this phenomenon has been numerically reported by Roshdi et al., [1, 2] and recently by Yang et al.,[3]. Wegner et al.,[4] parametric study examines the effects of distribution coefficient, droplet diameter, viscosity ratio, and STC gradient factors on mass transfer in the presence of Marangoni convection. In their parametric study, the effects of factors were individually studied reporting the strong effect of droplet size, and the interactive effects of parameters were ignored. Roshdi et al.,[5] parametric study investigated the interactive effects of parameters using response surface methodology instead of individual studying. They simultaneously studied the effects of several factors including distribution coefficient, viscosity ratio, density ratio, droplet diameter, and diffusivity ratio on the mass transfer and hydrodynamics. They concluded that the most effective factors are the distribution coefficient and viscosity ratio in mass transfer. Liu et al.,[6] studied the effects of nonlinear uniaxial extensional flow on single drop mass transfer reporting two times increase in Sherwood number in the presence of extensional flow due to the generation of new circulation zones inside the droplet.

The effects of several factors on LLE performance have been experimentally studied. Saien and Daliri[7] reported the enhanced effect of temperature in mass transfer due to an increase in diffusivity. Dehkordi et al., [8] reported the negative effects of contaminants due to the anionic-charged interface by contaminants and consequently the repulsion of dissociated anions of succinic acid. Saien and Ashrafi reported the enhanced effects of small amounts of salts in mass transfer due to the hydration of ions which favors solute to be transferred easier in the solvent [9]. Saien and Daneshamooz[10] reported that the ultrasonic waves compensated the deteriorating effects of hydrophilic nanoparticles on mass transfer. Dhindsa et al.,[11] reported the enhanced effect of hydrophobic SiO2 nanoparticles on mass transfer by the reason of Brownian motion of nanoparticles. Roshdi et al., also reported the deteriorating effects of hydrophilic nanoparticles on mass transfer due to the accumulation of nanoparticles in interfacial area and their barrier effect against the mass transfer[12].

Numerical investigation of mass transfer in single droplets or bubbles requires capturing the very thin mass boundary layer which is not possible in the static domain and moving droplet, hence moving reference frame configuration (MRF) should be applied. Another important challenge is that in mass transfer modeling, there is no direct access to interfacial nodes in the volume of fluid (VOF) approach to attach interfacial mass transfer boundary conditions. In the following sections, these two important issues have been addressed. The literature review summarized the numerical/ experimental studies reporting the effects of different factors on mass transfer and hydrodynamics. As can be seen, there is no study to investigate the STC effects on mass transfer and hydrodynamics of a single droplet system. Variations in STC value severely influence the hydrodynamics. The results of the present study will address the following research question: Do enormous hydrodynamic changes by STC disturb mass transfer?

2. Research Method

2.1. Governing equations

The VOF method suggested by Hirt and Nichols[13], was applied to capture the interface. In this approach, single momentum and continuity equations are solved for two immiscible fluids:

$$\frac{\partial \rho}{\partial t} + \nabla . \rho \boldsymbol{U} = 0 \tag{1}$$

$$\frac{\partial (\rho \boldsymbol{U})}{\partial t} + \nabla . \rho \boldsymbol{U}\boldsymbol{U} = -\nabla P + \nabla . \mu (\nabla \boldsymbol{U} + \nabla \boldsymbol{U}^T) + \rho \boldsymbol{g} + \boldsymbol{F_{SF}} \tag{2}$$

The mixture density and viscosity are defined as:

$$\rho = \alpha\rho_c + (1-\alpha)\rho_d \quad (3)$$

$$\mu = \alpha\mu_c + (1-\alpha)\mu_d \quad (4)$$

The motion of interface motion can be captured as:

$$\frac{\partial\alpha}{\partial t} + (\boldsymbol{U}.\nabla\alpha) = 0 \quad (5)$$

In Eq.2, the F_{SF} term is the surface tension force and is evaluated by the continuum surface stress (CSS) model[5].

The droplet center of mass velocity is calculated as below[14]:

$$V_{cm,y} = \frac{\sum_{i=1}^{n}\alpha_i V_i v_i}{\sum_{i=1}^{n}\alpha_i V_i} \quad (6)$$

In which $V_{cm,y}$ is the center of mass velocity in the y direction, α_i is the volume fraction of droplet in the i^{th} cell, V_i is the i^{th} cell volume and v_i is the velocity in the y-direction for the droplet phase.

Shape changes in the drops are commonly evaluated by aspect ratio. At the aspect ratio value of 1, drops are spherical while the values less than 1, show the oblate drops.

In the present study, the aspect ratio was obtained from Eq. 7, where, the X_{min}, X_{max}, y_{min}, and y_{max} were the maximum and minimum values of the droplet elemental positions in the x and y directions, and X_{min} is zero in the current axisymmetric conditions[14].

$$AR = \frac{y_{max} - y_{min}}{2(x_{max} - x_{min})} \quad (7)$$

Two interfacial boundary conditions are defined for mass transfer. The thermodynamic equilibrium forces the discontinuity at the interface and is given by Eq. 8:

$$\frac{C_d}{C_c} = K \quad (8)$$

Where K is the distribution coefficient.

The second boundary condition causes the continuity of solute flux at both sides of the interface and is represented by Eq. 9.

$$D_d\,\frac{\partial C_d}{\partial n} = D_c\,\frac{\partial C_c}{\partial n} \quad (10)$$

Using two interfacial boundary conditions in the mass transfer equation, the relation between the two phases is established in solute transfer. This challenging task has been solved in the following manner as previously conducted by Haroun et al.[15]:

$$C = \alpha C_c + (1-\alpha)C_d \quad (10)$$

Where C, C_c and C_d are the mixture, continuous phase, and dispersed phase concentrations, respectively. The single field mass transfer formulation is represented as [5, 15]:

$$\frac{\partial C}{\partial t} + \nabla.(\boldsymbol{U}C) = \nabla.\left(D_m(\nabla C)\right) + \nabla.\left(-D_m\frac{1-K}{\alpha + K(1-\alpha)}C\nabla\alpha\right) \quad (11)$$

In the above equation, D_m is expressed as below [5, 15]:

$$D_m = \frac{D_d D_c}{\alpha D_d + (1-\alpha)D_c} \quad (12)$$

After solving Eq. 11, the dispersed phase concentration is calculated from the following equation[5]:

$$C_d = \frac{C}{\left(\frac{\alpha}{K} + (1-\alpha)\right)} \quad (13)$$

The average concentration of droplet phase (C_d), is calculated from Eq.14 and used through simulations[5]:

$$\bar{C}_D = \frac{\sum_{i=0}^{n}\alpha_i V_i C_i}{\sum\alpha_i V_i} \quad (14)$$

where, C_i is the i_{th} cell concentration in the droplet phase, V_i is the i^{th} cell volume, and α_i is the volume fraction of the droplet in the i^{th} cell. The details were fully demonstrated in our previous study[5].

2.2. Boundary conditions and simulation setup

The model assumptions are listed below:

1. The incompressible, Newtonian, and immiscible fluids were considered in the present study.
2. Droplets were in circulating and oscillating regimes.

3. The solute (acetone) was soluble in both water and toluene phases.
4. Low solute concentration was assumed, hence the thermophysical properties were not influenced by the solute transfer.
5. The solute transferred from the droplet to the continuous phase
6. Zero initial solute concentration was assumed in the droplet phase.
7. Vertical droplet movement was considered.

The precise hydrodynamic simulations need a hydrodynamic boundary layer thickness of about d/80, while an accurate mass transfer model needs a boundary layer thickness less than d/5120, where d is the droplet diameter. The required computational domain for the simulation of liquid droplets is shown in Figure 1 with a width of 8d and a height of 12d to get domain-independent results.

As can be seen from Figure 1, if the whole domain has fine grids smaller than d/5120, the computational cells and time enormously increase and the problem will be unsolvable. To overcome this issue, the grid should be refined only in the zone near the droplet to reach the sufficient thickness of the mass transfer boundary layer. For this reason, the MRF approach was used in this study and is shown in Figure 1.

In the MRF approach, the droplet position is almost fixed at the domain center and the domain moves with the droplet center of mass velocity (Figure 1), hence finer grid zone position is fixed and attached to the droplet. In the case of the static domain and moving droplet, a very large domain is needed to capture the whole rise time; consequently, the finer grid zone becomes large, and the computational time increases.

To set MRF conditions, first the droplet center of the mass velocity was calculated from Eq.6 using computational codes. It was set exactly as domain velocity in opposite direction at the next step. Referring to Figure 1, domain boundaries include velocity inlet boundary at the top and moving wall boundary at the right in axisymmetric geometry. The center of mass velocity of the droplet was set as the velocity of both of them. At the domain bottom, an outflow boundary (zero gradients) was assumed (Figure 1). The details of the MRF approach have been explained in previous research [5].

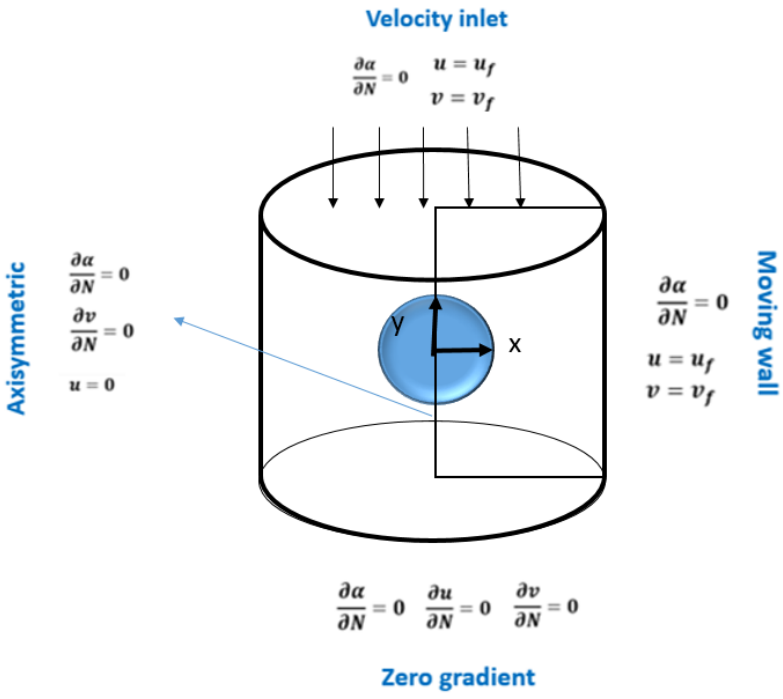

Figure 1. Computational domain with boundary conditions

The grid structure is shown in Figure 2 and magnified around the droplet to clarify. It can be seen that the grids have different levels of refinement inside the circles to reach less computational time and accurate prediction of boundary layer thickness. Referring to Table 1, the radius of five circles around the droplet are 4R, 3R, 2R, 1.5R, and 1.25R from the outer to the inner circle respectively, where R is the droplet radius. The initial uniform grid structure has the grid size of d/20, while the grid size inside the first outer circle is d/80 which are specified as level 0 and level 1 grid refinements in Table 1. Similarly, the grid sizes are d/320, d/1280, d/ 5120, and d/ 20480 inside the circles with the radius of 3R, 2R, 1.5R, and 1.25R respectively in Table 1. It can be seen from Table 1 that the grid refinement level has changed from level 1 to level 5 from outer to inner circle in Figure 1.

In the present study, toluene-rising droplets containing acetone were simulated in quiescent water, where acetone transferred from toluene into water. The system properties are given in Table 2.

The present work was aimed to investigate the STC effect on mass transfer and hydrodynamics. The properties mentioned in Table 2 were used in numerical experiments with different STC values shown in Table 3.

ANSYS Fluent 16 software with different types of user-defined functions including mass transfer model, MRF approach, and parallel processing codes were used through the simulations.

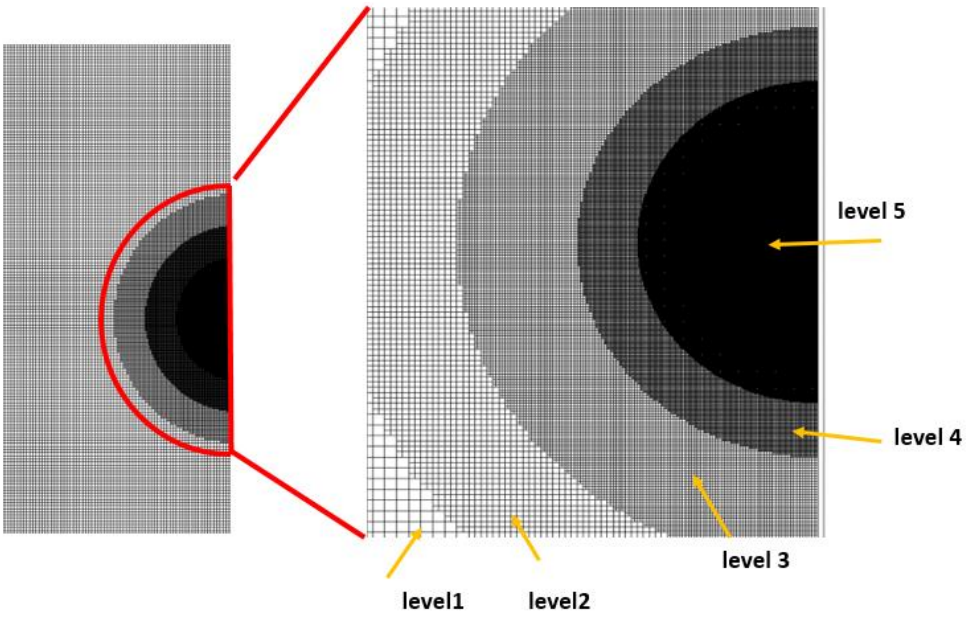

Figure 2. Grid structure in MRF approach

Table 1. Grid structure and refinement levels

Grid refinement level	Circle radius around the droplet	Grid size inside a circle (m)	Total cells number
Level 0	-	d/(20)	19200
Level 1	4R	d/(80)	26736
Level 2	3R	d/(320)	43962
Level 3	2R	d/(1280)	73854
Level 4	1.5R	d/(5120)	141720
Level 5	1.25R	d/(20480)	330204

Table 2. LLE system properties [1]

	Dispersed phase	Continuous phase
Density (kg/m3)	862.3	997.02
Dynamic viscosity (Pa.s)	$5.520*10^{-4}$	$8.903*10^{-4}$
Diffusion coefficient (m^2/s)	$2.9*10^{-9}$	$1.25*10^{-9}$
Distribution coefficient (-)	0.63	
Surface tension coefficient (N/m)	0.035	

Table 3. Simulations with different STC

Run number	Interfacial tension value(N/m)
1	0.0001
2	0.0005
3	0.001
4	0.035 (the base case-toluene)

3. Results and Analysis

3.1. hydrodynamic verification

To verify the hydrodynamic model, different sizes of toluene droplets were simulated ranging from spherical to oscillating regime, and the terminal velocities were obtained from Eq. 6 and are shown in Figure 3.

It can be seen that in the droplet size ranging from 0.5 to 8 mm, terminal velocity increases due to an increase of buoyant force (As forward force) against the drag and gravity forces (as opposing force). After that, the reduction in terminal velocity happens. In large droplets, the drag coefficient and interfacial area simultaneously increase and lead to an increase in drag force. On the other side, with the increase of droplet diameter, gravity force also increases. Simultaneous increase of drag and gravity forces decrease the terminal velocity[16].

Terminal velocity values of the present model in comparison with experimental data and correlations are shown in Figure 4 which show good agreement.

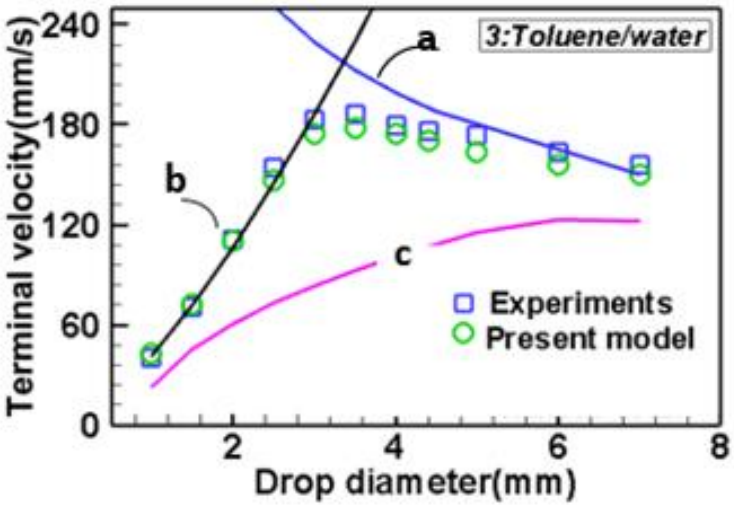

Figure 3. Terminal velocity of droplets in the present model and comparison with a) Thorsen et al. correlation[17], b) Hamielec et al. correlation[18], and c) Grace et al. correlation[19], and experimental data of Wegener et al.[20]

3.2. Grid independence study and mass transfer model verification

To obtain the grid-independent results, five grid refinement levels were used according to Table 1. It can be seen that, in large grid size (level 1), the mass transfer rate is high in every droplet diameter (Figures 4a and 4b). This is because the large grid size around the interfacial area, forces a large thickness of the mass boundary layer to the system, hence sharp concentration gradients virtually happen while they do not exist in real. It can be seen from Figure 4 that, with further grid refinement from level 4 to level 5, the results get closer to each other and tend to literature results. Additional grid refinement (finer than level 5) was not possible due to high computational time. This limitation has also been reported in previous studies[21]. In the present study, level 5 grid (Table1) was used due to the accurate capture of thin boundary layer and good verifications with previous studies [21-23].

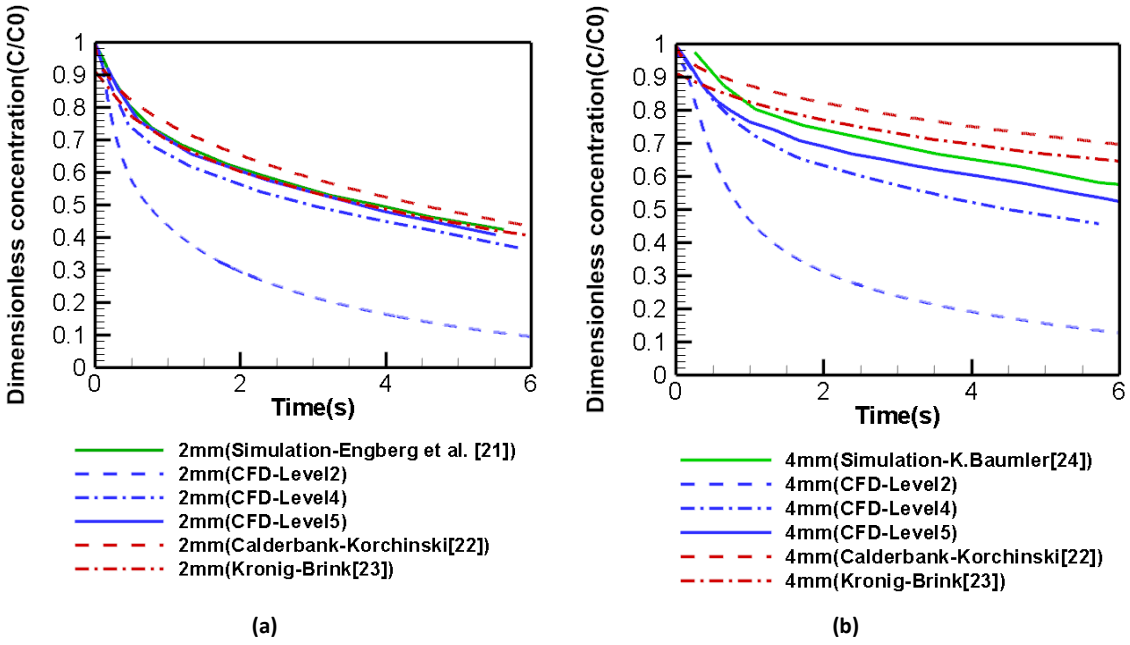

Figure 4. Verification of mass transfer model and mesh independence study for a) toluene droplet of 2mm size, b) toluene droplet of 4 mm size

The verification results of the mass transfer model have been given in Figure 4. The results of the current study were compared with the literature model [21, 24] and correlations[22, 23] demonstrated good agreement. Calderbank and Korchinski [22] and Kronig and Brink[23] correlations were developed in circulating droplets and the results of the present study agree well with them. In mentioned correlations, the STC effects on mass transfer were ignored which is the subject of the current research.

3.3. The STC effects on mass transfer and hydrodynamics

The STC effects on velocity profiles are shown in Figure 5a. It can be seen that with the reduction of STC from 0.1 to 0.0005, the reduction in transient velocity occurs until in STC of 0.0001 N/m, the breakage happens. STC reduction reduces surface tension force as a resistive force against the droplet deformation; hence, spherical droplets become oblate. In moving droplets as explained in section 3.1. three forces

determine the steady-state terminal velocity [16]. These are buoyant, drag, and gravity forces. With the reduction in STC, gravity and buoyant forces are constant, while, shape change from spherical to oblate increases the interfacial area and then drag force as an opposing force, hence the reduction in terminal velocity occurs. This conclusion is shown in Figure 5a.

The STC effects on the aspect ratio are demonstrated in Figure 5b. It can be seen that, while 2mm droplets are in the circulating regime (Figure 3), with the reduction of STC, the regime changes from circulating to oscillating occur. The oscillations appear in both terminal velocity and aspect ratio values (Figures 5a and b).

The STC effects on mass transfer profiles have been shown in Figure 5c. It can be seen that along with the decrease in STC values, the mass transfer rate firstly decreases (at the period of 1s from the starting point of simulations) and then increases. Referring to Figure 5a, Run2 and 3 have smaller velocities with respect to Run4, hence it is expectable that the mass transfer rate is lower in systems with small STC values due to the lower velocity and weakening of the mass transfer. However, after 1s, Run 2 and 3 have a higher mass transfer rate with respect to toluene droplets (Run4). This is because, with the reduction in STC, shape changes in droplets take place which alter the spherical droplets to oblate with the regime change from circulating to oscillating (Figure 5a). Oblate droplets (Run2 and 3) have a larger interfacial area to the same size of spherical droplets (Run1), which compensate the adverse effect of terminal velocity reduction in lower STC. Referring to Figure 5c, after 1s, the increase in mass transfer rate is observable in Run 2 and 3 results with respect to Run1 due to the increase of interfacial area, which is another important factor in mass transfer. The droplet shape variations with STC changes is shown in Figure 6.

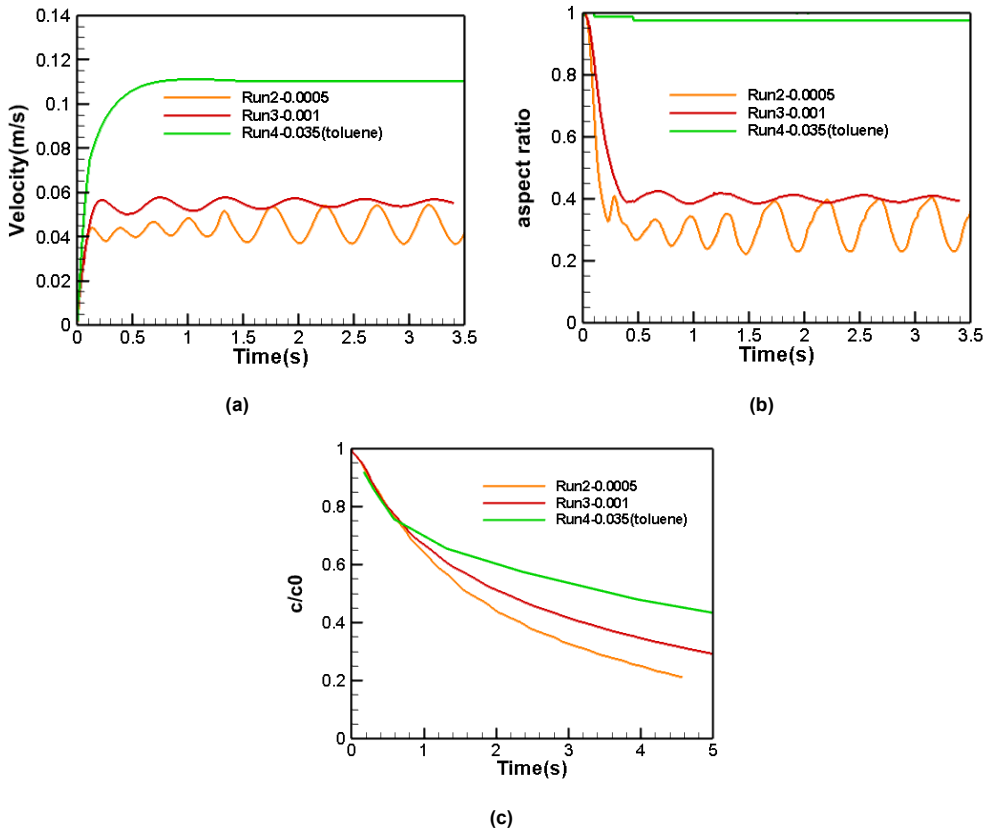

Figure 5. The effects of STC on a) transient velocity, b) aspect ratio, and c) concentration profiles of liquid-liquid extraction droplets

3.4. The STC effects on concentration profiles and droplet shapes

The STC effects on droplet shapes and concentration profiles are given in Figure 6. It can be seen that almost all of the droplets have spherical shapes at the initial rise times; however, depending on STC values, shape changes occur after a while. In Run 1 (Figure 6a) with the smallest STC, severe shape changes start after 0.1 s from the initial rising time, but in Run 4 (Figure 6d) with the largest STC, changes do not happen. This result is also observable in Figure 5b, where the aspect ratio of run 4 is around 0.98 which confirms the spherical shape at whole rising time in the STC of 0.035. It can be seen from Figure 6a that, after about 0.24s, droplet breakage happens. Continuous vertical to horizontal diameter changes (Aspect ratio in Eq. 7), cause aspect ratio oscillations (Figure 5b), these changes are also observable in droplet shapes in Figure 6b and c. In low STC values, the recirculating zone is formed just behind the droplets (Figure 6b and c), while they do not exist in circulating droplets (Figure 6d). Concentration profiles of acetone are shown in Figure 6a-d with numbered legends. The mass transfer direction is from droplet to continuous phase. Concentration profiles show that the solute transfer due to convective mass transfer takes place at the droplet behind, hence it reduces the concentration values around the droplet and then inside. Inside the droplets, among streamlines, the mass transfer mechanism is diffusion with a lower rate with respect to the convective mass transfer, hence high concentration cores inside the droplets appear and negatively influence the mass transfer and remain in whole rising time (Figure 6b-d). In oblate droplets (Figure 6b and c), the recirculating zone behind the droplets retards the mass transfer, which does not exist in Figure 6d. Results of Figure 5c showed that the increase of interfacial area in oblate droplets (Figure 6b and c) compensates the effects of negative influencing factors in the mass transfer including the reduction of velocity and the formation of recirculation zones.

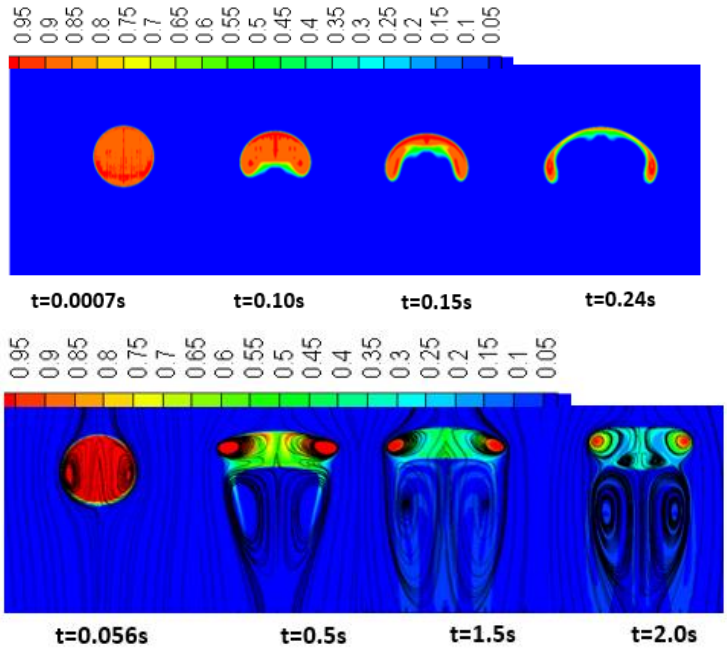

a)

Run1: STC=0.0001 N/m

b)

Run2: STC=0.0005 N/m

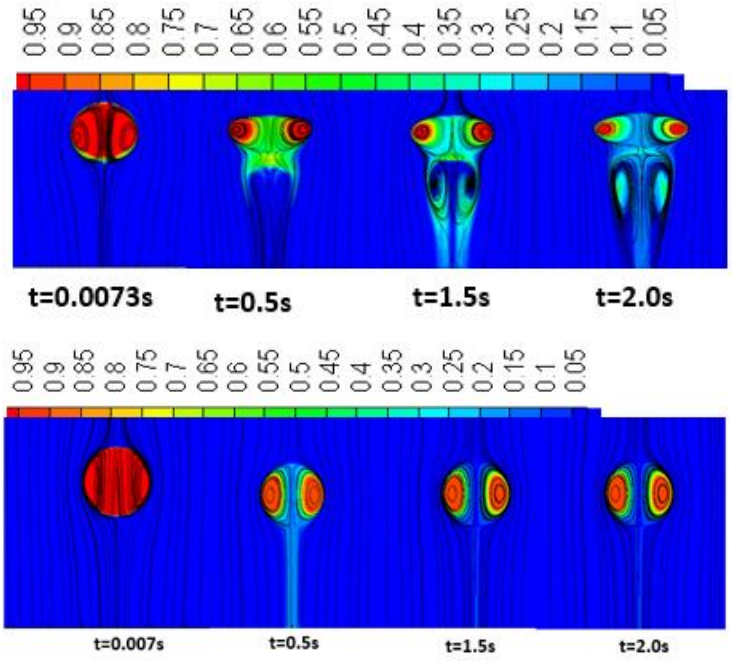

c)

Run3: STC=0.001 N/m

d)

Run4: STC=0.035 N/m (toluene)

Figure 6. The effects of STC on droplet shapes, concentration profiles, and streamlines of a) Run1, b) Run2, c) Run3, d) Run4

4. Conclusion

In the present study, the microscopic mass transfer model of LLE droplets was developed. This model type has many applications in studying the effects of different parameters on the performance of LLE single droplet systems and then large-scale LLE columns. The important conclusions of the present study can be listed as below:

1. The MRF approach of the present study can be applied in both bubble and droplet systems, in LLE and absorption processes. The advantage of MRF is the ability to refine the grid size to the smallest degree to capture the very thin mass boundary layer as well as the hydrodynamic boundary layer with less computational time.
2. VOF approach and single field mass transfer model in parallel processing mode have been used in hydrodynamic and mass transfer simulations in the MRF zone. This general type of mass transfer model can be applied in other applications like the absorption and falling film.
3. In hydrodynamic simulations, with the reduction in STC, spherical droplets become oblate, terminal velocity decreases, and the regime change from circulating to oscillating takes place, and the recirculating zone just behind the droplet is formed. The oscillating regime characteristics are oscillations in aspect ratio and velocity values.
4. In mass transfer simulations, with the reduction in STC values, the mass transfer rate increases due to the increase of interfacial area despite the reduction in velocities and the formation of recirculating zones behind the droplets.
5. The results of the present study showed how the LLE system acts when surface tension reduces while other physical properties are kept constant. Similar to this behavior will happen when surface active agents are added to LLE. The reduction in terminal velocity, the regime changes from circulating to oscillating, and variations in mass transfer values will take place, but the quantities need additional investigation.

As can be seen, STC has a significant effect on both hydrodynamics and mass transfer; hence, the next step of the present study will be the investigation of the simultaneous effects of STC with other affecting factors like density, viscosity, and diffusivity of both

phases as well as the distribution coefficient and droplet diameter using the design of experiment methods.

Nomenclature

C	Concentration, kg/m^3
D	Diffusion coefficient, m^2/s
D_m	Mixture diffusivity, m^2/s
d	Droplet diameter, m
$\boldsymbol{F_{SF}}$	Surface tension force, N/m3
g	Gravitational acceleration, m/s^2
K	Distribution coefficient
P	Pressure, kg/ms^2
R	Droplet radius (m)
n	Normal vector
t	Time, s
U	Velocity vector, m/s
V	Cell volume (m^3)
u	X-velocity component, m /s
v	Y-velocity component, m/s
X	X-axis of domain, m
Y	Y-axis of domain, m
Greek letters	
μ	Dynamic viscosity, Pa.s
σ	Surface tension coefficient, N/m
ρ	Density, kg/m^3
α	Volume fraction
Subscripts	
c	Continuous phase
d	Dispersed phase, droplet
cm	Center of mass
min	Minimum
max	Maximum
Abbreviations	
VOF	Volume of fluid
STC	Surface tension coefficient
MRF	Moving reference frame
LLE	Liquid-liquid extraction
CSS	Continuum surface stress

References

1. S. Roshdi, N. Kasiri, A. Rahbar-Kelishami, Simulation of Marangoni convection effects on the hydrodynamics of liquid–liquid extraction drops, Chemical Engineering Communications, 206(12) (2019) 1628-1644.
2. M. Wegener, T. Eppinger, K. Bäumler, M. Kraume, A. Paschedag, E. Bänsch, Transient rise velocity and mass transfer of a single drop with interfacial instabilities—numerical investigations, Chemical Engineering Science, 64(23) (2009) 4835-4845.
3. Q.-J. Yang, Q. Mao, W. Cao, Numerical simulation of the Marangoni flow on mass transfer from single droplet with different Reynolds numbers, Colloids and Surfaces A: Physicochemical and Engineering Aspects, 639 (2022) 128385.
4. M. Wegener, A numerical parameter study on the impact of Marangoni convection on the mass transfer at buoyancy-driven single droplets, International Journal of Heat and Mass Transfer, 71 (2014) 769-778.
5. S. Roshdi, N. Kasiri, Coupling VOF interfacial mass transfer model with RSM approach in LLE systems: Developing the new correlations for mass transfer, aspect ratio and terminal velocity, International Communications in Heat and Mass Transfer, 123 (2021) 105216.
6. A. Liu, J. Chen, M. Guo, C. Chen, M. Yang, C. Yang, The internal circulations on internal mass transfer rate of a single drop in nonlinear uniaxial extensional flow, Chinese Journal of Chemical Engineering, (2022).
7. J. Saien, S. Daliri, Improving performance of liquid–liquid extraction with temperature for mass transfer resistance in both phases, Journal of the Taiwan Institute of Chemical Engineers, 45(3) (2014) 808-814.
8. A.M. Dehkordi, S. Ghasemian, D. Bastani, N. Ahmadpour, Model for Excess Mass-Transfer Resistance of Contaminated Liquid− Liquid Systems, Industrial & engineering chemistry research, 46(5) (2007) 1563-1571.
9. J. Saien, F. Ashrafi, Mass transfer enhancement in liquid−liquid extraction with very dilute aqueous salt solutions, Industrial & Engineering Chemistry Research, 48(22) (2009) 10008-10014.
10. J. Saien, S. Daneshamoz, Compensating effect of ultrasonic waves on retarding action of nanoparticles in drops liquid–liquid extraction, Ultrasonics sonochemistry, 41 (2018) 514-520.
11. A. Dhindsa, A. Sobti, R. Wanchoo, A.P. Toor, Study on mass transfer using nanofluid drops in liquid-liquid extraction column, International Communications in Heat and Mass Transfer, 136 (2022) 106194.
12. S. Roshdi, N. Kasiri, A. Rahbar-Kelishami, Deterioration effects of SiO2 nanoparticles on the mass transfer in a single drop system with resistance in both phases, International Communications in Heat and Mass Transfer, 139 (2022) 106470.
13. C.W. Hirt, B.D. Nichols, Volume of fluid (VOF) method for the dynamics of free boundaries, Journal of computational physics, 39(1) (1981) 201-225.
14. S. Roshdi, N. Kasiri, A. Rahbar-Kelishami, VOF simulation of single rising drops in three liquid-liquid extraction systems using CSF and CSS interfacial force models, Brazilian Journal of Chemical Engineering, 35 (2018) 1315-1331.
15. Y. Haroun, D. Legendre, L. Raynal, Volume of fluid method for interfacial reactive mass transfer: application to stable

liquid film, Chemical Engineering Science, 65(10) (2010) 2896-2909.
16. M. Wegener, N. Paul, M. Kraume, Fluid dynamics and mass transfer at single droplets in liquid/liquid systems, International Journal of Heat and Mass Transfer, 71 (2014) 475-495.
17. G. Thorsen, R. Stordalen, S. Terjesen, On the terminal velocity of circulating and oscillating liquid drops, Chemical Engineering Science, 23(5) (1968) 413-426.
18. A. Hamielec, S. Storey, J. Whitehead, Viscous flow around fluid spheres at intermediate Reynolds numbers (II), The Canadian Journal of Chemical Engineering, 41(6) (1963) 246-251.
19. J. Grace, T. Wairegi, T. Nguyen, Shapes and velocities of single drops and bubbles moving freely through immiscible liquids, Trans. Inst. Chem. Eng, 54(3) (1976) 167-173.
20. M. Wegener, M. Kraume, A.R. Paschedag, Terminal and transient drop rise velocity of single toluene droplets in water, AIChE journal, 56(1) (2010) 2-10.
21. R.F. Engberg, M. Wegener, E.Y. Kenig, The impact of Marangoni convection on fluid dynamics and mass transfer at deformable single rising droplets–A numerical study, Chemical Engineering Science, 116 (2014) 208-222.
22. P. Calderbank, I. Korchinski, Circulation in liquid drops:(A heat-transfer study), Chemical Engineering Science, 6(2) (1956) 65-78.
23. R. Kronig, J. Brink, On the theory of extraction from falling droplets, Applied Scientific Research, 2(1) (1951) 142-154.
24. K. Bäumler, Simulation of single drops with variable interfacial tension, Phd thesis,Faculty of Natural Sciences at the Friedrich-Alexander University of Erlangen-Nuremberg, Germany, (2014).

نشریه فناوری نفت، گاز و پتروشیمی، ۱۰(۲): ۱۳۷-۱۲۵، بهار و زمستان ۱۴۰۲

مقاله تحقیقاتی

مدل‌سازی میکروسکوپی انتقال جرم در سیستم‌های LLE با استفاده از رویکرد: VOF اثرات کشش سطحی بر انتقال جرم و هیدرودینامیک

سپیده رشدی[۱،*]، نوراله کثیری[۲]

۱. گروه مهندسی شیمی، دانشکده فنی، دانشگاه ارومیه، ارومیه، ایران

۲. مرکز مهندسی فرآیند به کمک کامپیوتر، دانشکده مهندسی شیمی نفت و گاز، دانشگاه علم و صنعت ایران، نارمک، تهران، ایران

مشخصات مقاله

تاریخچه مقاله:

دریافت: ۳ اسفند ۱۴۰۱

دریافت پس از اصلاح: ۶ مرداد ۱۴۰۲

پذیرش نهایی: ۳۱ مرداد ۱۴۰۲

کلمات کلیدی:

دیدگاه حجم سیال

انتقال جرم

استخراج مایع-مایع

دستگاه مختصات متحرک

کشش سطحی

هیدرودینامیک

*عهده‌دار مکاتبات؛ سپیده رشدی

رایانامه:

s.roshdi@urmia.ac.ir

تلفن: ۰۴۴۳۲۷۷۵۶۶۰

چکیده

استخراج مایع-مایع یکی از اصلی ترین فرآیندهای جداسازی است که کاربردهای فراوانی در صنایع مختلف دارد. از میان پارامترهای مختلف موثر بر عملکرد مایع- مایع، اثر کشش سطحی در مطالعه حاضر مورد بررسی قرار گرفته است که قبلا بررسی نشده‌است. انتقال جرم یک سیستم تک قطره با استفاده از تلفیق رویکرد حجم سیال با رویکرد انتقال جرمی تک میدانی شبیه‌سازی شده است. با توجه به زمان محاسباتی بالا، رویکرد مرجع مختصات متحرک در حالت پردازش موازی به کدهای محاسباتی اضافه شده‌است که در آن قطره ساکن و دامنه محاسباتی متحرک فرض می‌شود. نتایج نشان داد که با کاهش ضریب کشش سطحی، در حالی که سایر پارامترها ثابت نگه داشته می‌شوند، تغییر رژیم از کروی به نوسانی رخ می‌دهد، سرعت کاهش می‌یابد و با کاهش بیشتر در ضریب کشش سطحی، شکست قطرات اتفاق می‌افتد. با وجود کاهش قابل توجه در سرعت حدی، کاهش انتقال جرم مشاهده نشد. زیرا همزمان با کاهش کشش سطحی، افزایش سطح انتقال جرم اتفاق می‌افتد که به نفع انتقال جرم است در حالی که کاهش سرعت، به ضرر آن است. کانتورهای غلظت قطرات در ضرایب کشش سطحی مختلف در رژیم مختلف قطرات با شروع از چرخشی تا رژیم شکست قطره گزارش شده‌است..

نحوه استناد به این مقاله:

Roshdi S, Kasiri N., Microscopic Modeling of Mass Transfer in LLE Systems Using VOF Approach: The Surface Tension Effects on Mass Transfer and Hydrodynamics, Journal of Oil, Gas and Petrochemical Technology, 2023; 10(2): 125-137. DOI:10.22034/JOGPT.2023.386913.1112.